5-1-2022

BIOMECHANICAL PROPERTIES OF PORCINE NEONATAL EPIDERMIS FROM FORELIMB TISSUE IN THE LONGITUDINAL AND CIRCUMFERENTIAL DIRECTIONS

Neaz Almir

BIOMECHANICAL PROPERTIES OF PORCINE NEONATAL EPIDERMIS FROM FORELIMB TISSUE IN THE LONGITUDINAL AND CIRCUMFERENTIAL DIRECTIONS

by

NEAZ ALMIR

Presented to the Faculty of the Honors College of

The University of Texas at Arlington in Partial Fulfillment

of the Requirements

for the Degree of

HONORS BACHELOR OF SCIENCE IN BIOMEDICAL ENGINEERING

THE UNIVERSITY OF TEXAS AT ARLINGTON

May 2022

ACKNOWLEDGMENTS

I thank Dr. Jun Liao for allowing me to use his lab facility and equipment to perform my research. Specifically, for providing me permission to use the Uniaxial Testing Machinery, the necessary measuring calipers, the storage facilities, and the neonatal tissues that were used in this study. I also would like to thank Dr. Alan Taylor Mark for mentoring me during my research at the lab at the University of Texas at Arlington and training me in the usage of the lab equipment and lab safety. Moreover, I deeply appreciate the Department of Biomedical Engineering for providing the resources and space for me to conduct my research.

To both of my parents, relatives, and friends who have supported me either morally or financially, I extend my deepest appreciation to them.

April 22, 2022

ABSTRACT

BIOMECHANICAL PROPERTIES OF PORCINE NEONATAL EPIDERMIS FROM FORELIMB TISSUE IN THE LONGITUDINAL AND CIRCUMFERENTIAL DIRECTIONS

Neaz Almir, B.S. Biomedical Engineering

The University of Texas at Arlington, 2022

Faculty Mentor: Jun Liao

In adult humans, it is common to replace damaged tissues and epidermal tissues of smooth muscles on internal organs with porcine xenografts during a surgical procedure. However, there is little research on the usage of neonatal porcine tissues because of the difficulty in performing mechanical testing and obtaining samples from neonatal pigs due to the delicate property of the tissues. By performing mechanical testing on tissues obtained from stillborn pigs, we can calculate the amount of stress and strain these tissues undergo and how these tissues can be used to replace epidermal tissues in limbs of human infants. Using a Uniaxial Machine, measurements of stress relaxation, creep, and pull to failure will be calculated for various porcine tissues in the longitudinal and circumferential

directions. The data will be analyzed to determine the average maximum stresses and strains these tissues can undergo for various tensile loadings before the tissues fail.

TABLE OF CONTENTS

LIST OF ILLUSTRATIONS

LIST OF TABLES

CHAPTER 1

INTRODUCTION

1.1 Background

About half a million patients in the United States require treatments for burns, and there are approximately 40,000 hospitalized patients and 3,400 deaths (Yamamoto et al., 2018). Xenografts are known as the transplantation of animal cells and tissues to a human recipient. Genetically engineered pigs have been produced to minimize and inhibit the development of complement proteins that cause an immune reaction in the human recipient. The purpose of using porcine tissues is due to the nearly identical biomechanical properties to human tissues than any other species. This is an excellent solution to the transplant shortage of human tissues for patients who suffered infections that resulted in skin loss, deep penetrating burns, closing large, open wounds, skin cancer, and even treating pressure injuries and skin sores. In addition, there is a lack of excised human epidermal tissues that can be used for biomechanical research in (Ranamukhaarachchi et al., 2016). Because of these factors, there is a need for further research on the biomechanical properties of porcine tissues to understand how they can be used to replace and function identically to native human tissue.

The usage of adult pig tissues in xenotransplantation procedures has always been the primary focus for these procedures. However, a study was conducted that discovered the properties of porcine neonatal skin tissues for the application of skin transplants. Neonatal fibroblasts, which are a type of epidermal cell in neonatal tissues, were shown to

enhance the wound healing property in the patient (Paul, 2008). Because of the healing nature of neonatal tissues, its applications as a form of xenotransplantation to human recipients should be considered. However, neonatal pig tissues differ in biomechanical property due to the collagen fiber density and orientation, making it imperative to identify the mechanical behavior when neonatal pig tissues are under various strains and loading.

Some of the most common locations where tissue is removed from the donor is from the buttocks, back, upper arm, and inner thigh (Coull, 1991). The skin in these locations is very thick and collagenous, and hence is why neonatal pig forelimb epidermis is an acceptable choice to study its biomechanical properties for these applications. In a study comparing the biomechanical properties of forelimbs and hindlimbs of porcine tissues, it was found that inverse dynamics revealed that the peak horizontal reaction force exerted by the forelimbs was greater than hindlimbs (Thorup et al., 2007). Moreover, during a gait analysis, the forelimbs were shown to carry more of the body weight as well as receive higher peak ground reaction forces than the hindlimbs. In addition, the hindlimbs stance phase was shorter than that of the forelimbs, showing the increased resistance to stress deformation upon loading and ensuring it is a reliable test sample to use for the purposes of this experiment.

1.2 Biomechanics and Nature of Human Skin

Human skin is a heterogenous and anisotropic living material, which means it is composed of three different layers from the inner to the outer dermis due to the three different orientations of the collagen fibers. Hence, depending on the direction and orientation of the skin, it will exhibit different mechanical properties in two directions: the circumferential and longitudinal directions. Thus, when a load is applied, the collagen

fibrils in the skin will orient in the applied direction of the uniaxial in proportion to stresses and strains. Stress is equivalent to the applied force over the area of the skin, while the strain is the change in the length of the skin over its fixed length, or how easily the skin can change its dimension due to applied loading. These values of stress and strain can be calculated using a Uniaxial Testing Machine by performing the following functions to gather data points in calculation for the mean stress and strain: preconditioning, stress relaxation, creep, and pull to failure. Preconditioning is an imperative process in biomechanical testing where the material is continually stretched and relaxed in cycles to allow the elastic energy to dissipate as heat into the environment. This will prevent any incorrection in the data acquisition of the other three following tests. Stress relaxation occurs when the material is stretched to a position and maintained at the position for 15 minutes. The machine plots the loss in stress in the material over time. Creep occurs when a constant loading is applied to a material and causes a slowly increasing change in its strain. Once the data sets are obtained, the tissue samples will be examined for their stresses and strains in pull to failure, the normalized stress for stress relaxation, and the normalized strain for creep in the longitudinal and circumferential directions.

A T-test will be performed at the end of the study to determine if the data is statistically significant between the circumferential and longitudinal directions for each of the three tests of stress relaxation, creep, and pull to failure. If the calculated p-value is determined to be less than 0.05, then the data is statistically significant and there is a difference in the stress and strain behavior of the tissues in the longitudinal and circumferential directions. If this is the case, then the tissues are proven to be anisotropic in character and therefore closely resemble human tissues. If the p-value is greater than

0.05, then the data is not statistically significant, and the neonatal porcine tissues are not suitable for usage in epidermal xenotransplantation.

CHAPTER 2

MATERIALS AND METHODOLOGY

A still born pig was obtained from the slaughterhouse and brought to the laboratory to undergo dissection. The forelimbs from the pig have been isolated from the rest of the cadaver as depicted in the image below (Figure 2.1). Using a scalpel, the skin was separated from the muscle tissue by ensuring that none of the muscle tissue became destroyed or remained adhered to the epidermis (Figure 2.2). The remaining muscle components of the forelimb and the rest of the carcass were preserved to be used in other future experiments.

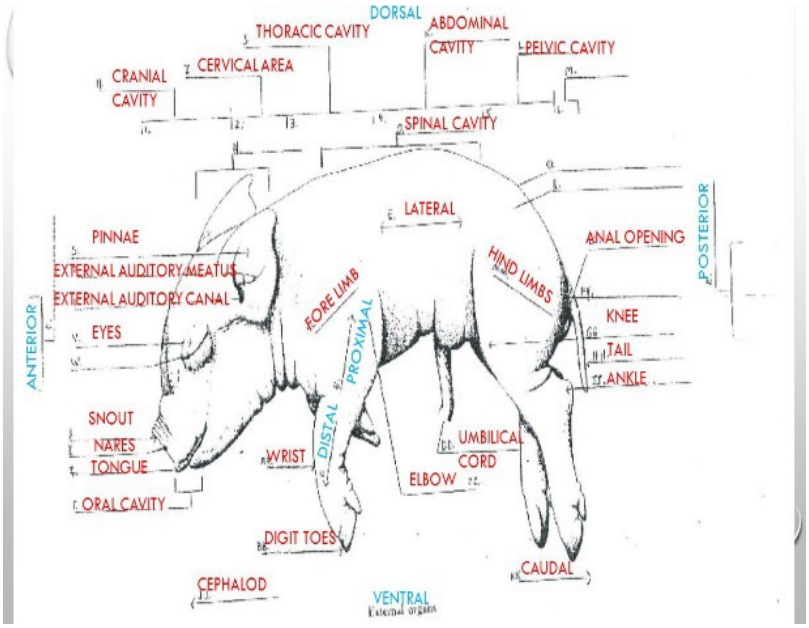

Figure 2.1: Diagram of Pig Anatomy Displaying Forelimbs

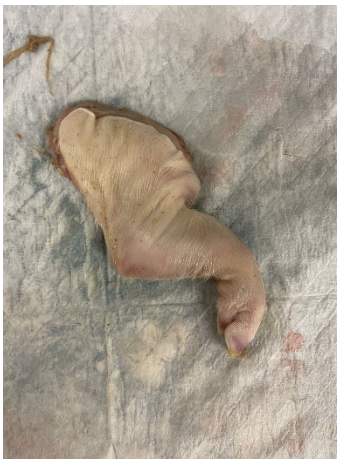

Figure 2.2: Whole Neonatal Pig Forelimb

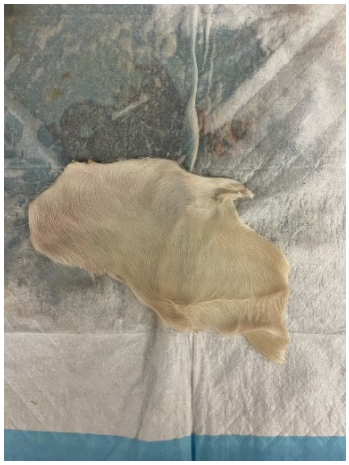

Figure 2.3: Excised Forelimb Skin

It is important to note that once the skin was removed, it was positioned in the same fashion as it had been attached to the muscle tissue. Using the scalpel, five samples were cut in the longitudinal direction and another five samples were cut in the circumferential direction of the pig tissue. Using a digital caliper, the samples were measured and cut to be approximately 40 mm in length and 10 mm in width (Figure 2.4). The samples were stored in the samples cups and labeled appropriately. Afterwards, the samples were stored in a –20-degree Celsius fridge until testing was to begin.

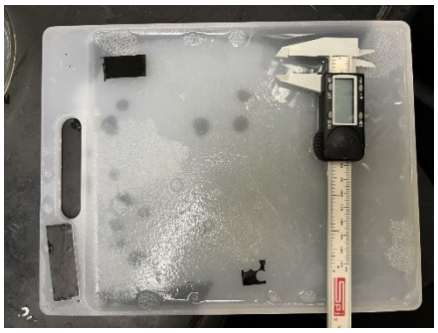

Figure 2.4: Digital Caliper and Cutting Board for Tissue Samples

To start the testing, the samples were thawed for about one hour in a warm water bath (Figure 2.5). Once thawed, the samples were removed from the sample cups and were prepared one by one for testing. First, the following information was obtained using a digital caliper to determine the exact dimensions of the samples: width, length, thickness, and the grip-to-grip value. The grip-to-grip value is the distance between the clamps in the uniaxial machine once the tissue sample is placed and fastened to the clamps (Figure 2.6). PBS was continually sprayed on the sample to ensure the tissue did not dry out during the experiment.

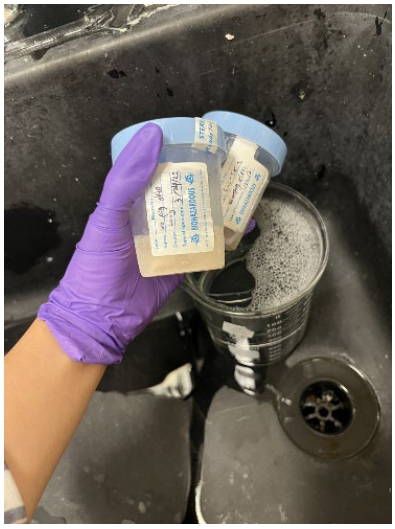

Figure 2.5: Thawing Samples

Figure 2.6: Sample in Uniaxial Machine

First, the longitudinal samples of forelimb tissue were placed one by one in the uniaxial machine for testing. Each sample undergoes the four testing modalities of preconditioning, stress relaxation, creep, and pull to failure. The “R Controller Software” was used to compute the data and plot the changes in the stress and strain over the time inputted by the user. Under the “Test Procedures” menu, the preconditioning test was selected (Figure 2.7).

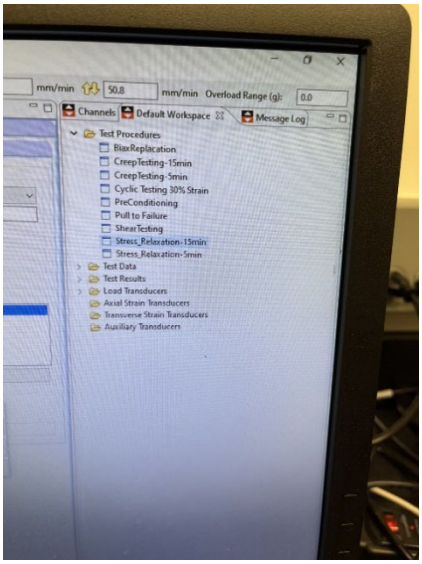

Figure 2.7: Test Procedures

Next, under the “Acquisition” tab, the name of the data set was titled “NeonatalPorcineSkin_Long1_preconditioning,” where “long” represents the sample from the longitudinal direction, “1” represents the sample number, and “preconditioning” specifies the test that was done on that sample (Figure 2.8).

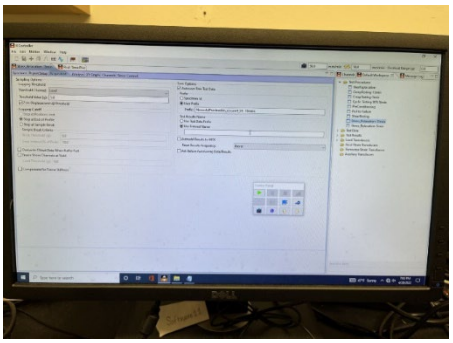

Figure 2.8: Acquisition Tab

Next, under the “Servocontrol” tab, the desired parameters must always be set for only the preconditioning test. We need to specify how many millimeters we want the Uniaxial machine to pull the tissue for every 20 seconds. To calculate this value, it is ten percent of the grip-to-grip value. This value is typed into the “desired parameters” section. Finally, the play button is selected, and the Uniaxial machine will automatically record and save the data in a Microsoft Excel file. For the other three tests of stress relaxation, creep, and pull to failure, no other parameters need to be calculated and typed into the system. Every time a new test is conducted, the name of the data set is changed to specify the test type, the sample number, and whether the sample was from the longitudinal or circumferential direction. The same process was performed for the other five samples in the circumferential directions and the data was automatically saved by the R-Controller Software into Excel files.

CHAPTER 3

RESULTS

The following data listed in this section depicts the analyzed data for all ten tissue samples in the longitudinal and circumferential directions. For the analysis of stress relaxation, each sample was maintained at a load of 100 N until the maximum loading had been reached. The normalized stresses were plotted over time and recorded in an excel sheet. Using the excel spreadsheet formulas, the percent change for stress relaxation and creep for all samples was done by subtracting the final normal stress from the initial stress (value = 1) multiplied by 100, and the final normal strain from the initial strain (value = 1) multiplied by 100, respectively. The data analysis was purposely conducted to obtain the values of percent change of stress relaxation and creep for the circumferential and longitudinal directions because these values will be used to perform the T-test depicted in Table 3.5. In addition, the graphs for these tests for all ten samples are depicted to verify the accuracy of the data depending on if the graph shows an exponential growth or decay.

Conversely, the tests on the longitudinal and circumferential directions for pull to failure provided the computation of the average time it took each sample to break. Similarly, the average maximum stresses that the samples experienced upon failure were computed in addition to the average strains, extensions, of the samples when they failed. The strain of interest in this case is the normalized strain, which is the calculated strain divided by the yield strain to produce a true, accurate strain value. These values are helpful

to perform a T-test between the average circumferential and longitudinal stresses and the average circumferential and longitudinal strains as depicted in Table 3.6. Below are the tables and corresponding graphs that depict the information described in this section.

Table 3.1: Average Values of Time, Stress, Strain, and Normalized Strain of Longitudinal Samples for Pull to Failure

Time (s)	Stress (Mpa)	Strain	Normalized Strain
94.89999771	408.27	0.980483002	1.980483002
26.70000076	656.956	0.294450795	1.294450795
140.0999756	1006.672	23.3344	140.0999756
49.00006104	82.01279	0.564757716	1.564757716
17.1496582	107.5429	0.187289725	1.187289725
65.56993866	452.2906	5.072276248	29.22539136

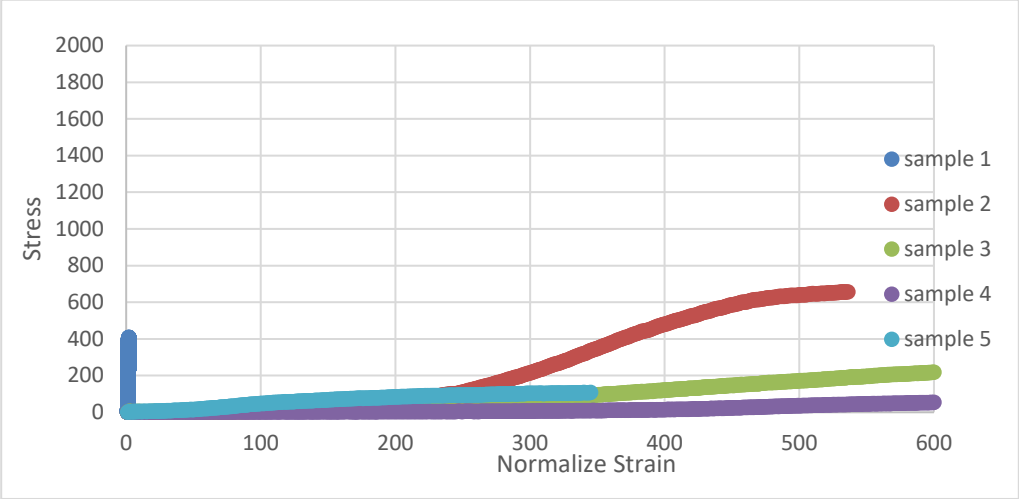

Figure 3.1: Scatter Plot for Longitudinal Pull to Failure

Table 3.2: Average Values of Time, Stress, Strain, and Normalized Strain Of Circumferential Samples for Pull to Failure

Time (s)	Stress (Mpa)	Strain	Normalized Strain
78.5	306.6878	0.522778	1.52277772
41.65	207.6668	0.330122	1.330121667
41.65	269.0774	0.463406	1.463406083
68.15	53.18986	0.783774	1.783774361
48.161	564.7757	0.37934	1.379339572
55.6222	280.2795	0.495884	1.49588388

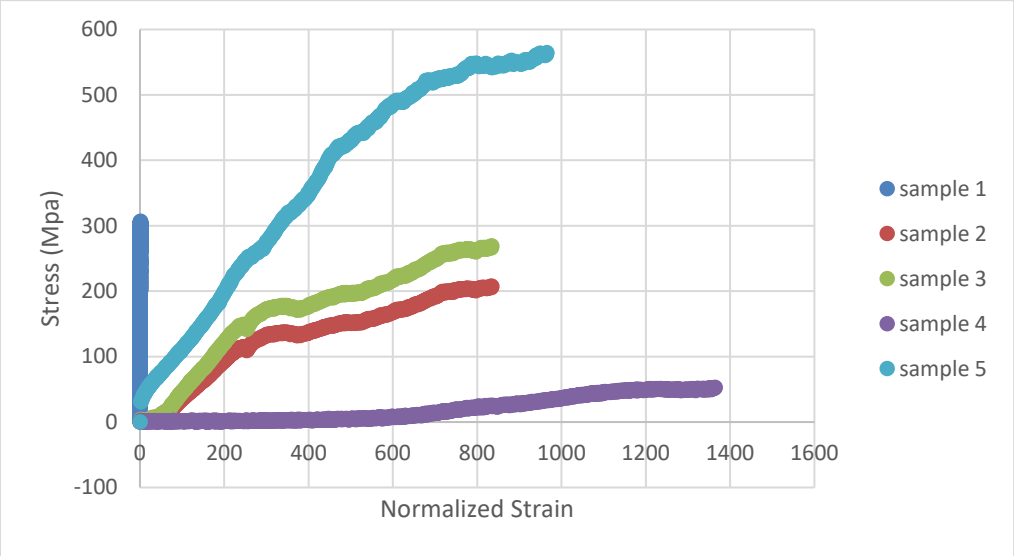

Figure 3.2: Scatter Plot for Circumferential Pull to Failure

Table 3.3: Percent Change of Stress Relaxation for Longitudinal and Circumferential Directions

% Change in Stress Relaxation Longitudinal Samples		% Change in Stress Relaxation Circumferential Samples	
Sample #	Percent Change in the Samples	Sample #	Percent Change
1	71.79099952	1	78.57575858
2	59.7826056	2	85.18064938
3	70.43530972	3	85.18064938
4	63.4745234	4	68.8739706
5	69.25892008	5	84.73539287
Average	66.94847166	Average	80.50928416
Stand. Dev.	5.10794089		7.082060852

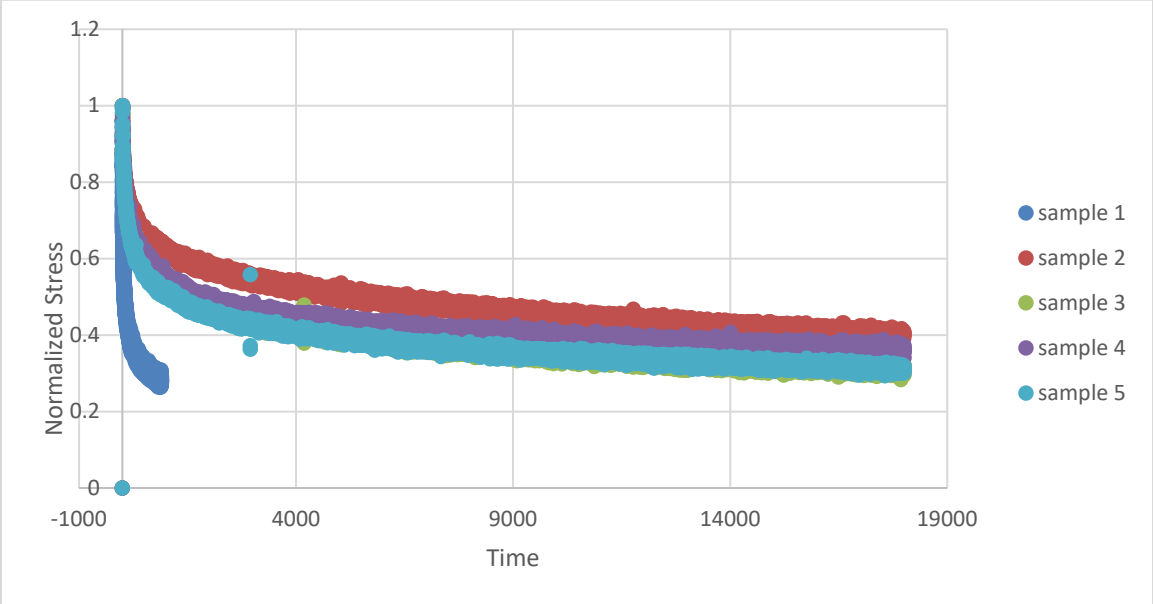

Figure 3.3: Scatter Plot for Longitudinal Stress Relaxation

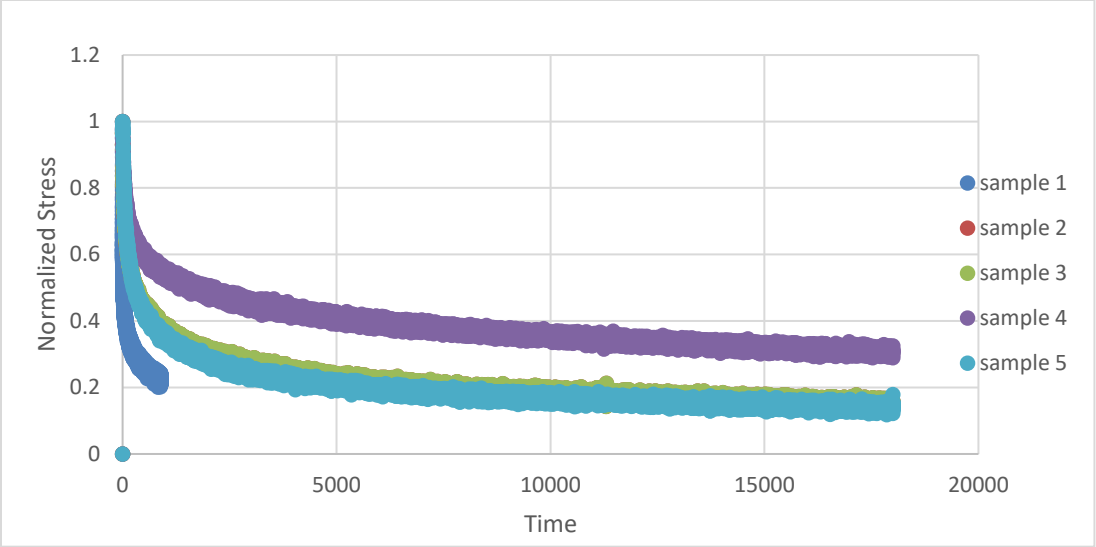

Figure 3.4: Scatter Plot for Circumferential Stress Relaxation

Table 3.4: Percent Change of Creep for Longitudinal and Circumferential Directions

% Change in Creep Longitudinal Samples		% Change in Creep Circumferential Samples	
Sample #	Percent Change in the Samples	Sample #	Percent Change in the Samples
1	22.37247767	1	11.9048
2	6.244598013	2	2.620729
3	5.543749526	3	3.678831
4	42.89266207	4	20.21045
5	4.078318689	5	19.54848
Average	16.22636119	Average	11.59266
Stand. Dev.	16.65979498	Stand. Dev.	8.37829

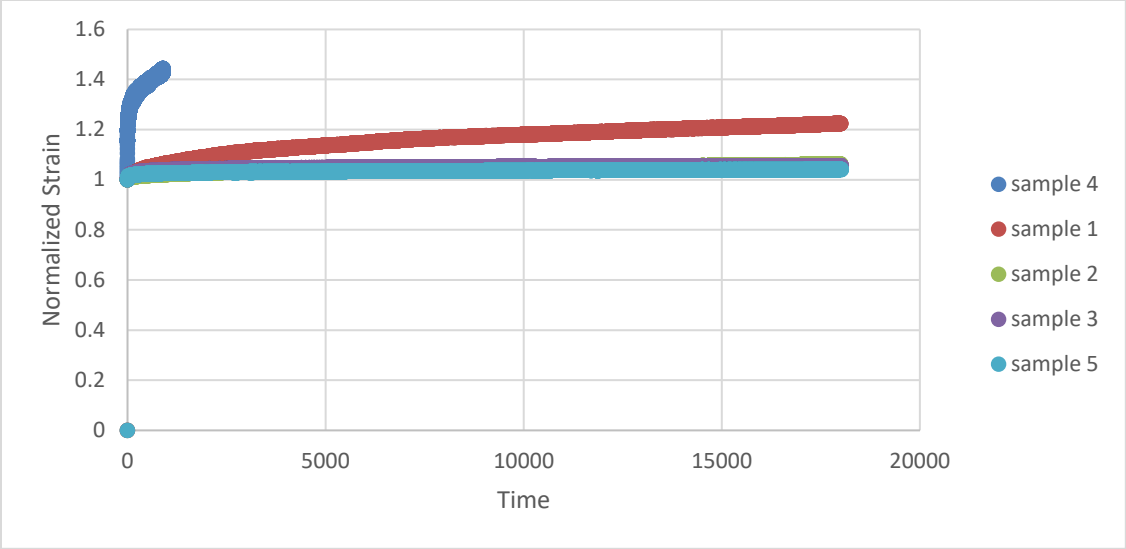

Figure 3.5: Longitudinal Values for Creep

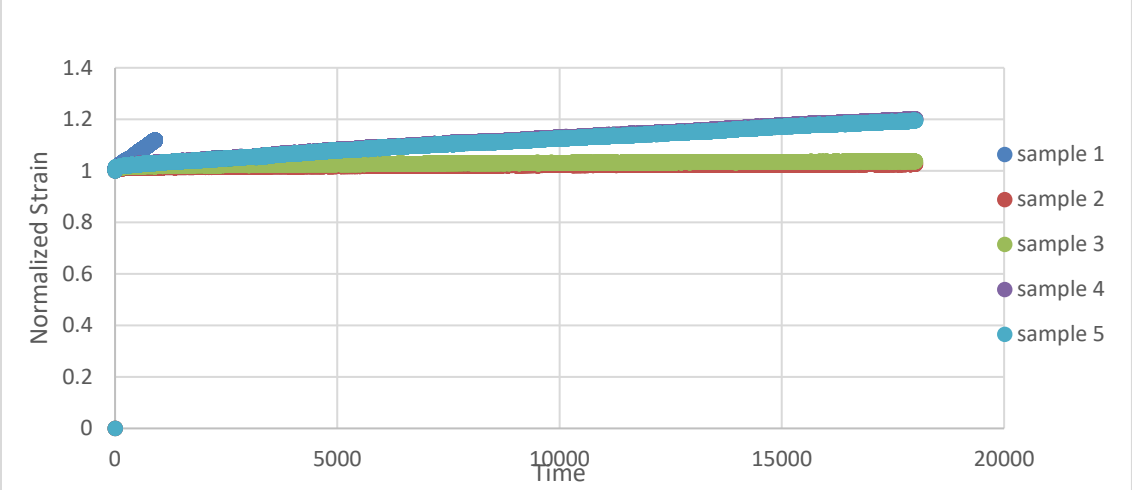

Figure 3.6: Circumferential Samples for Creep

Table 3.5: T-Tests Comparing Longitudinal and Circumferential Directions of Stress Relaxation and Creep

T-Test Stress Relaxation			T-Test Creep		
Sample #	% Change Longitudinal	% Change Circumferential	Sample #	% Change Longitudinal	% Change Circumferential
1	71.79099952	78.57575858	1	22.37247767	11.9048
2	59.7826056	85.18064938	2	6.244598013	2.620729
3	70.43530972	85.18064938	3	5.543749526	3.678831
4	63.4745234	68.8739706	4	42.89266207	20.21045
5	69.25892008	84.73539287	5	4.078318689	19.54848
P-value	0.008409997		P-value	0.593659588	

Table 3.6: T-Tests Comparing Longitudinal and Circumferential Directions of Pull To Failure for Stress and Strain

	T-Test Pull to Failure Stress			T-Test Pull to Failure Strain	
Sample #	Circumferential	Longitudinal	Sample #	Circumferential	Longitudinal
1	306.6878	408.2699946	1	0.52277772	0.980483
2	207.6668234	656.9560135	2	0.330121667	0.294451
3	269.0773926	1006.6715	3	0.463406083	23.3344
4	53.18985954	82.01278941	4	0.783774361	0.564758
5	564.7757343	107.5429335	5	0.379339572	0.18729
P-value	0.399031341		P-value	0.345785004	

CHAPTER 4

DISCUSSION AND CONCLUSION

4.1 Discussion of Graphical Data

Upon analysis of the provided graphs for pull to failure (Figure 3.1 and Figure 3.2), we can conclude that the tests conducted for both the circumferential and longitudinal directions are accurate and have little to no error. This conclusion can be drawn because as time increases, the stress rises gradually, reaches a peak, and then gradually starts to decrease. The reason for the increase in stress is due to the increasing load on the sample, which occurs in the linearly elastic region of the graph. Once the sample reaches the maximum stress it can endure before failure, known as the peak stress, the sample starts to experience permanent failure, known as plastic deformation. Plastic deformation onset of the sample is exhibited when the stress on the graph begins to decrease because the sample ripped, and no longer can handle an increasing applied load.

Moreover, the same conclusions can be drawn for the graphs of stress relaxation (Figures 3.3 and 3.4) and creep (Figures 3.5 and 3.6). Upon examination of the graphs for stress relaxation, the stress exhibits an exponential decay in the stress as time increases. Because the samples are being extended and held at one length for fifteen minutes, the stress, or the force, the sample experiences decrease over time since the energy is lost as heat. In addition, upon examination of the graphs for creep, all the samples display an increase in the normalized strain as time increases. Therefore, the samples have an

exponential growth in the strain since the sample's length gradually increases over time due to a constant loading applied.

4.2 Explanation of Statistical Significance of Data

There were four T-tests that were performed. For all tests, a two-tailed sample equal variance T-test was performed since we are determining if there is any difference between the comparison of two groups, and if the data occurs due to the trend or randomly. The first test compared the statistical significance of stress relaxation for the circumferential and longitudinal directions (Table 3.5). A p-value of 0.008 was produced for this test, and because $0.008 < 0.05$, there is a statistical difference for the stress relaxation test for both directions. These results describe the mechanical property of the neonatal epidermal tissues in that the collagen fibers exhibit a greater percent change in the circumferential direction, 80.51 ± 7.08, as opposed to the longitudinal direction 66.95 ± 5.11 (Table 3.3). In the circumferential direction, the tissues show a greater reduction of stress over time due to energy dissipation under a constant strain.

The second test compared the statistical significance of creep for the circumferential and longitudinal directions (Table 3.5). In contrast to stress relaxation, the creep test produced a p-value of 0.59, showing there was no statistical difference between the circumferential and longitudinal directions. For the longitudinal direction, the percent change in creep is 16.22 ± 16.65, and 11.59 ± 8.37 in the circumferential directions (Table 3.4). This means that the tissues exhibit the same properties of creep and displacement when under a constant loading.

Finally, the last two tests determined if there was a statistical significance for pull to failure by comparing the stresses in the circumferential and longitudinal directions and

the strains for the circumferential and longitudinal directions (Table 3.6). The calculated p-value was 0.40 for the stress analysis and 0.34 for the strain analysis, proving that there was no statistical significance and no difference between the longitudinal and circumferential average normalized stress and the longitudinal and circumferential average normalized strain. Longitudinal and circumferential samples fail at the same stresses and strains due to excessive loading.

4.3 Conclusions

The results from the study confirm the anisotropic behavior of neonatal porcine epidermal tissues, allowing for the possibility of these tissues to be used in epidermal xenotransplantation procedures for humans. Neonatal tissues contain neonatal stem cells and growth factors that could significantly reduce the time for tissue regrowth in humans. Epidermal tissues exhibit anisotropic behavior depending on the location of the tissue in the body, and the use of forelimb epidermal tissue allows it to be transplanted to areas that are usually subject to high mechanical loading, which was proven by the significant difference for stress relaxation (Nickell et al., 2000). The strong resistance to extension and creep of these tissues is due to the layering and multi-orientation of the collagen fibers in the epidermis, dermis, and hypodermis. Skin is also described as non-linear and viscoelastic, meaning that the material has a high resistance to elongation and strain and will snap back to its original state once loading is removed (Annaidh et al., 2012). This goes to explain why the skin experiences the same behavior and resistance to creep as described earlier in the results section, and as to why when the skin fails, it fails in all directions.

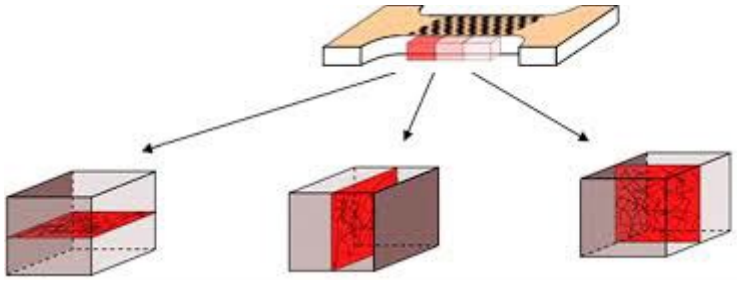

Figure 4.1: Anisotropic Property of Skin

For future studies on this topic, one should investigate the biomechanical properties of neonatal porcine tendon and their applications for their potential use in xenotransplantation. By understanding the biomechanical properties of various types of neonatal porcine tissues, this opens the door for an opportunity that combats against the current donor shortage.

REFERENCES

Coull A (1991) Making sense of split skin graft donor sites. Nurse Times 87(40): 52–4.

Paul C. N. (2008). Skin substitutes in burn care. Wounds: a compendium of clinical research and practice, 20(7), 203–205.

Ranamukhaarachchi, S. A., Lehnert, S., Ranamukhaarachchi, S. L., Sprenger, L., Schneider, T., Mansoor, I., Rai, K., Häfeli, U. O., & Stoeber, B. (2016). A micromechanical comparison of human and porcine skin before and after preservation by freezing for medical device development. Scientific Reports, 6(1). https://doi.org/10.1038/srep32074

Ní Annaidh, A., Bruyère, K., Destrade, M., Gilchrist, M. D., & Otténio, M. (2012). Characterization of the anisotropic mechanical properties of excised human skin. Journal of the mechanical behavior of biomedical materials, 5(1), 139–148. https://doi.org/10.1016/j.jmbbm.2011.08.016

Nickell, S., Hermann, M., Essenpreis, M., Farrell, T. J., Krämer, U., & Patterson, M. S. (2000). Anisotropy of light propagation in human skin. Physics in medicine and biology, 45(10), 2873–2886. https://doi.org/10.1088/0031-9155/45/10/31

Thorup, V. M., Tøgersen, F. A., Jørgensen, B., & Jensen, B. R. (2007). Biomechanical gait analysis of pigs walking on solid concrete floor. Animal, 1(5), 708–715. https://doi.org/10.1017/s1751731107736753

Yamamoto, T., Iwase, H., King, T. W., Hara, H., & Cooper, D. (2018). Skin xenotransplantation: Historical review and clinical potential. Burns: journal of the International Society for Burn Injuries, 44(7), 1738–1749. https://doi.org/10.1016/j.burns.2018.02.02

BIOGRAPHICAL INFORMATION

During Neaz's undergraduate career as a tissue biomedical engineer, she has been involved in career development opportunities such as a Product Safety Intern at Mary Kay and as a research assistant at Cook Children's studying brain patterns in 5–6-year-olds with Cerebral Palsy. These opportunities have expanded her knowledge in both the industrial and clinical settings, in which she was required to conduct three cell culture experiments per week, use imaging technologies to produce brain scans of patients and filter these images using MATLAB. While working as a Product Safety Intern at Mary Kay, she performed three-four experiments of cell culture for fibroblasts and keratinocytes and evaluated for cell viability and proliferation using an MTT assay. In addition, weekly reports were conducted (15 pages) using chemical safety and toxicology government databases that described the chemicals used in a product and information about their usage in other Class 2 cosmetic products that have already been FDA approved. As a Graduate research assistant for Cook Children's, Neaz studied motor and sensory controls in patients with cerebral palsy using brain stimulation with TMS. Brain information processing was done using MEG, high density EEG, and TMS. Data and imaging scans were processed using MATLAB. Neaz intends to graduate with a Master of Science in Biomedical Engineering (Imaging) in Spring 2023. Afterwards, she would pursue a position in healthcare where she would like to apply her skills in designing her own laboratory research and putting together projects for her team to accomplish, including the planning and execution for these projects.